An Analytic BRDF Model of Canopy Radiative Transfer and Its Inversion

Shunlin Liang and Alan H. Strahler, *Member, IEEE*

Abstract— **Radiative transfer modeling of the bidirectional reflectance distribution function (BRDF) of leaf canopies is a powerful tool to relate multiangle remotely sensed data to biophysical parameters of the leaf canopy and to retrieve such parameters from multiangle imagery. However, the approximate approaches for multiple scattering that are used in the inversion of existing models are quite limited, and the sky radiance frequently is simply treated as isotropic. This paper presents an analytical model based on a rigorous canopy radiative transfer equation in which the multiple-scattering component is approximated by asymptotic theory and the single-scattering calculation, which requires numerical integration to properly accommodate the hotspot effect, is also simplified. Because the model is sensitive to angular variation in sky radiance, we further provide an accompanying new formulation for directional radiance in which the unscattered solar radiance and single-scattering radiance are calculated exactly, and multiple-scattering is approximated by the well-known δ two-stream approach. A series of validations against exact calculations indicates that both models are quite accurate, especially when the viewing angle is smaller than 55°. The Powell algorithm is then used to retrieve biophysical parameters from multiangle observations based on both the canopy and the sky radiance distribution models. The results using the soybean data of Ranson *et al.* to recover four of nine soybean biophysical parameters indicate that inversion of the present canopy model retrieves leaf area index well. Leaf angle distribution was not retrieved as accurately for the same dataset, perhaps because these measurements do not describe the hotspot well. Further experiments are required to explore the applicability of this canopy model.**

Index Terms—**Radiative transfer, bidirectional reflectance distribution function (BRDF), leaf canopy, biophysical parameters, sky radiance distribution, inversion.**

NOMENCLATURE

A^*	Spherical albedo of the canopy for multiple scattering.
δ	Dirac delta function.
$E(\cdot)$	Escape function in the canopy asymptotic reflectance.
f	Forward fraction of the scattering energy for the atmosphere.

Manuscript received May 12, 1992; revised November 13, 1992. This work was supported by the National Aeronautics and Space Administration under Grant NAGW-2082, Contracts NAS5-30917 and NAS5-31369, and the U.S. National Science Foundation under Grant INT-9014263.

The authors are with the Department of Geography and Center for Remote Sensing, Boston University, Boston, MA, 02215.

IEEE Log Number 9212146.

(Continued) NOMENCLATURE

F_{a0}	Extraterrestrial solar irradiance at the top of the atmosphere.
F_0	Extraterrestrial solar irradiance above canopy after penetrating the atmosphere.
g	Average asymmetric parameter of the one-term Henyey–Greenstein (OTHG) phase function.
g_a	Asymmetric parameter of the OTHG phase function for the aerosol.
g_c	Asymmetric parameter of the OTHG phase function for the canopy.
$\Gamma(\Omega', \Omega)$	Area scattering transfer function of the canopy.
$h(\cdot)$	Correlation function accounting for the hotspot effect.
i_0	Extraterrestrial solar net flux incident on the top of the canopy.
$I^{\pm}(\tau)$	Upward and downward integrated-radiance of the atmosphere.
$I^0(\tau, \Omega)$	Unscattered solar radiance.
$I^1(\tau, \Omega)$	Single-scattering radiance.
$I^M(\tau, \Omega)$	Multiple-scattering radiance.
$J(\tau, \Omega)$	Source function of the radiative transfer equation.
k	Leaf dimension parameter.
LAD	Leaf angle distribution.
LAI	Leaf area index.
μ_0	Cosine of the solar zenith angle θ_0.
n	Leaf wax refractive index.
$\Omega(\mu, \phi)$	Unit vector of the solid angle consisting of cosine of zenith angle μ and azimuth angle ϕ.
$P(\Omega', \Omega)$	Phase function of the atmosphere.
$p(\mu', \mu)$	Azimuth-independent phase function of the atmosphere.
ϕ_0	Solar azimuth angle.
r_l	Leaf hemisphere reflectance.
r_s	Reflectance of a Lambertian surface.
r_0	Reflectance of a Lambertian panel.
$R_0(\tau_c, \mu, \mu_0)$	Bidirectional reflectance of the canopy with the optical depth $\tau_c i$.
$R(\tau, \Omega, \Omega_0)$	BRDF of the canopy at optical depth τ.
t_l	Leaf hemisphere transmittance.
ω_c	Single-scattering albedo of the canopy.
ω_a	Single-scattering albedo of the aerosol.

0196–2892/93$03.00 © 1993 IEEE

I. Introduction

OFF-nadir measurements of the radiance of Earth surface features are now being acquired for small test sites by airborne sensors, such as the Advanced Solid-State Array Spectroradiometer (ASAS) [1], and will be acquired globally in the near future with the development of new satellite sensors, such as the Multiangle Imaging Spectroradiometer (MISR) [2]. An important area of theoretical studies on multiangle observations is the modeling of the directional reflective properties of the leaf canopy, since canopies reflect radiation anisotropically. For this purpose, a number of physical models have been developed in the past, and excellent reviews of these are now available in the literature [3], [4]. Easy invertibility of a canopy directional reflectance model is highly desirable, if we wish to retrieve various environmental and biophysical parameters from remotely sensed imagery. For this purpose, an analytic model is preferable. Several analytic directional-reflectance canopy models based on radiative transfer theory [5]–[8] have been published. The differences among these depend on their problem formulations and approximations for the multiple-scattering component. Most of these analytic models are based on the two-stream approximation or its variants, such as the Suits model [5], SAIL model [6], and other models [8], [9]. However, the approximate approaches for the calculation of multiple scattering are still quite limited. Numerical calculations [10] using the Gauss–Seidel algorithm show that the multiple-scattering component is over 50% of the total upwelling canopy radiance in the near-IR region, which is least affected by atmospheric scattering and therefore highly useful in the inversion of biophysical parameters from multiangle remotely sensed imagery. Therefore, further development of accurate approximation approaches for multiple scattering are very necessary. Verstraete *et al.* [11], [12], treated the canopy as a semi-infinite medium for multiple scattering, following Hapke's approach [13] for scattering by a planetary surface. The assumption of a semi-infinite medium is appropriate for a dust-covered surface, but does not sufficiently account for the canopy in some cases, especially when the canopy is optically thin. For example, Liang and Strahler [10] calculated from a specific parameter set that the difference in upwelling radiance between $LAI = 2.0$ and $LAI = 6.5$ is 10.2% above the canopy and 9.9% above a clear atmosphere in the near-IR region, and the difference between $LAI = 1.0$ and $LAI = 3.0$ is 33.9% above the canopy and 15.9% above a clear atmosphere in the red band.

In this study, we derive an approximate solution for the multiple-scattering component of a canopy radiative transfer equation based on asymptotic theory, in which the canopy is treated as an optically thick but vertically finite medium with the soil reflectance also incorporated into the formulation. The strategy is to divide the radiation field of the canopy into three components: unscattered sunlight, single-scattering radiance, and multiple-scattering radiance. According to this formulation, the unscattered solar radiance has an analytical solution and can be calculated directly. The single-scattering radiance needs to be evaluated by a numerical integration because of the explicit inclusion of the hotspot effect. Here an approximate formula for the single-scattering component is derived using a Taylor expansion. The multiple-scattering component is calculated by the asymptotic fitting technique. This decomposition enables us to obtain very accurate solutions. If the canopy is optically very thick, and the multiple-scattering component dominates, the asymptotic technique is very accurate, so the resulting accuracy will be high. If the canopy is optically thin, so that the multiple-scattering component is less important and the asymptotic technique less accurate, high accuracy is still achieved due to the exact single-scattering calculation. The canopy bidirectional reflectance distribution function (BRDF) is then easy to formulate after creating the explicit radiance calculation formulae of all components.

Most existing analytic canopy directional reflectance models have not incorporated sky radiance component in an effective manner [14], [3]. Either the canopy is completely decoupled from the atmosphere, or the downward radiance distribution is treated as isotropic. Actually, the sky radiance distribution is very anisotropic [10], [15]. Under normal atmospheric conditions, sky radiance will range from 5–40% of the total downward radiance [16]. There exist some analytic atmospheric radiative transfer models that can be used for sky radiance calculations. However, most of these are normally used for radiative flux calculations, for which the angular dependence is unimportant. In our new formulation, the radiation field of the atmosphere is also decomposed into three parts: unscattered solar radiance, single-scattering radiance, and multiple-scattering radiance. Only the multiple scattering component is approximated by the two-stream approach, and other two components are exactly calculated. This is appropriate since we mainly need to consider the clear atmosphere condition where the aerosol optical depth is small, and especially so in the near-IR bands that are most suited for the inversion.

A series of validations using different numerical solutions were carried out to test the approximation formulae. The results indicate that our analytic canopy BRDF model and sky radiance distribution model are accurate when the viewing angles are not too large. The Powell algorithm is then used to invert parameters characterizing canopy biophysical properties from the soybean data measured by Ranson *et al.* [16], which have been widely used in BRDF modeling studies.

II. A Canopy Radiative Transfer Model

Some earlier canopy radiative transfer formulations have assumed that the canopy has an isotopic scattering phase function [17]. However, theory and experiments have proven that the canopy scattering function is very anisotropic and is rotationally variant, i.e., the phase function depends not only on the scattering angle, but also on incident and outgoing directions [18]–[21]. In this study, a more rigorous canopy radiative transfer model has been used for the basis on which explicit formulae are derived. A brief description is given below; more details can be found elsewhere [10], [19], [20].

The one-dimensional radiative transfer equation of a horizontally homogeneous and infinite canopy is given by

$$-\mu\frac{\partial I(\tau,\Omega)}{\partial\tau}+h(\tau,\Omega)G(\Omega)I(\tau,\Omega)=\frac{1}{\pi}\int_{4\pi}\Gamma(\Omega'\to\Omega)I(\tau,\Omega')\,d\Omega' \quad (1)$$

with the boundary condition

$$I(0,\Omega)=\delta(\Omega-\Omega_0)i_0$$
$$I(\tau_c,\Omega)=\frac{r_s}{\pi}\int_{2\pi_-}|\mu'|I(\tau_c,\Omega')\,d\Omega' \quad (2)$$

where the unit vector Ω with an azimuth angle ϕ and a zenith angle $\theta=\cos^{-1}\mu$ with respect to the outward normal characterizes the solid angle; Ω_0 characterizes the incidence direction; i_0 is the incidence net flux ($F_0\pi$) above the canopy; r_s is the reflectance of a Lambertian background (e.g., soil) under the canopy; τ_c is the optical depth of the canopy; and $2\pi_-$ stands for the lower hemisphere. (The Nomenclature defines the major mathematical notation used in this test.)

In (1), the function $G(\Omega)$ is the mean projection of a unit foliage area in the direction Ω, the correlation function $h(\tau,\Omega)$ is used to account for the hotspot phenomenon, and the area scattering phase function $\Gamma(\Omega'\to\Omega)$ is defined as consisting of both diffuse and specular components. The detailed descriptions of these functions are provided in Liang and Strahler [10], and are based on work by Marshak [19], Shultis, and Myneni [20].

We decompose the radiation field into three parts: unscattered radiance $I^0(\tau,\Omega)$, single-scattering radiance $I^1(\tau,\Omega)$, and multiple-scattering radiance $I^M(\tau,\Omega)$

$$I(\tau,\Omega)=I^0(\tau,\Omega)+I^1(\tau,\Omega)+I^M(\tau,\Omega). \quad (3)$$

A simple schema is represented in Fig. 1. Uncollided radiance includes both downward unintercepted radiance and the upward radiance reflected once from the soil surface without further scattering. Single-scattering radiance has been scattered once by the canopy, and multiple-scattering radiance is scattered more than once by the canopy.

For unscattered solar radiance, the formulas are

$$I^0(\tau,\Omega)=\begin{cases}I_d^0(\tau,\Omega)=i_0\exp\left[-\frac{G(\Omega)\tau}{|\mu_0|}\right]\delta(\Omega-\Omega_0)\\ \quad\mu<0\\ I_u^0(\tau,\Omega)=i_0/\pi\exp\left[-\frac{G(\Omega_0)\tau_c}{|\mu_0|}\right]r_s\mu_0\exp\left[-\xi(\tau,\Omega)\right]\\ \quad\mu>0\end{cases} \quad (4)$$

where

$$\xi(\tau,\Omega)=\frac{1}{\mu}\int_\tau^{\tau_c}h(t,\Omega)G(\Omega)\,dt=G(\Omega)\frac{\tau_c-\tau}{\mu}-\left[\sqrt{\frac{G(\Omega_0)G(\Omega)}{\mu|\mu_0|}}\frac{kH}{\Delta(\Omega_0,\Omega)}\right]t_1. \quad (5)$$

Here t_1 is defined as

$$t_1=\exp\left[-\frac{\Delta(\Omega_0,\Omega)\tau}{kH}\right]-\exp\left[-\frac{\Delta(\Omega_0,\Omega)\tau_c}{kH}\right].$$

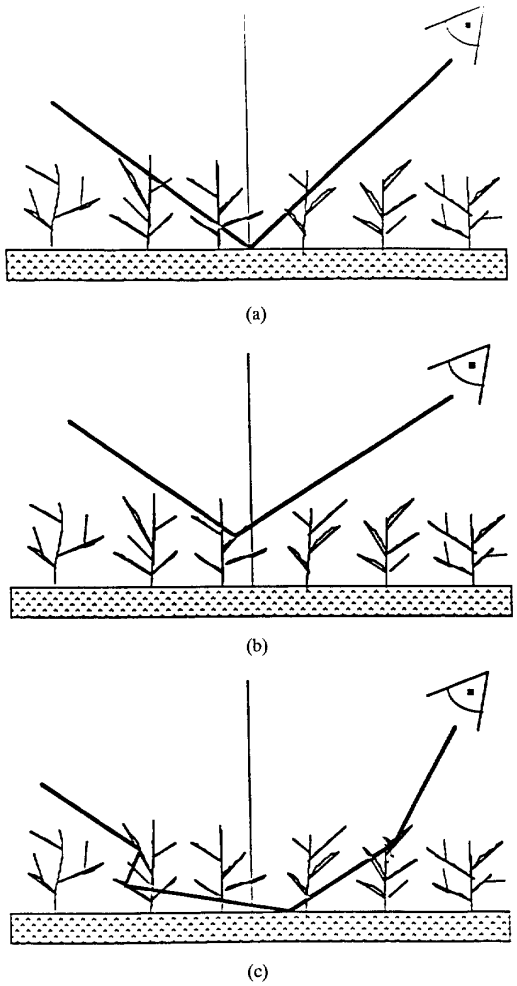

Fig. 1. The schema of the radiation field decomposition: (a) unscattered solar component, (b) single-scattering component, (c) and multiple-scattering component.

For the single-scattering radiance, the solution in the downward direction ($\mu<0$) can be easily written as

$$I^1(\tau,\Omega)=\begin{cases}\frac{\tau i_0\Gamma(\Omega_0\to\Omega)}{\pi|\mu_0|}\exp\left[-\frac{G(\Omega_0)\tau}{|\mu_0|}\right] & \mu=\mu_0\\ \frac{i_0|\mu_0|\Gamma(\Omega_0\to\Omega)}{\pi[G(\Omega)|\mu_0|-G(\Omega_0)|\mu|]}\cdot\left[\exp\left(-\frac{G(\Omega_0)\tau}{|\mu_0|}\right)-\exp\left(-\frac{G(\Omega)\tau}{|\mu|}\right)\right] & \text{otherwise.}\end{cases} \quad (6)$$

In the upward direction ($\mu>0$), the solutions are a little complicated because of the hotspot effect:

$$I^1(\tau,\Omega)=\frac{1}{\mu}\int_\tau^{\tau_c}F(\tau',\Omega)\cdot\exp\left[-\frac{1}{\mu}\int_\tau^{\tau'}h(\xi,\Omega)G(\Omega)\,d\xi\right]d\tau' \quad (7)$$

where the second integration in (7) can be explicitly obtained by means of (5) with an alternative integrand range, and

$$F(\tau', \Omega) = \frac{i_0}{\pi}\Gamma(\Omega_0 \rightarrow \Omega)\exp\left[-\frac{G(\Omega_0)\tau'}{|\mu_0|}\right]. \quad (8)$$

Now we begin to deal with the multiple-scattering radiance $I^M(\tau, \Omega)$. The radiative transfer equation and its boundary conditions are given by

$$-\mu\frac{\partial I^M(\tau, \Omega)}{\partial \tau} + G(\Omega)I^M(\tau, \Omega) = J(\tau, \Omega) \quad (9)$$

subject to boundary condition:

$$I^M(0, \Omega) = 0$$
$$I^M(\tau_c, \Omega) = \frac{r_s}{\pi}\int_{2\pi_-} |\mu'|[I^M(\tau_c, \Omega') + I^1(\tau_c, \Omega')]\, d\Omega'.$$

Here the source function is

$$J(\tau, \Omega) = \frac{1}{\pi}\int_{4\pi} \Gamma(\Omega' \rightarrow \Omega)[I^M(\tau, \Omega') + I^1(\tau, \Omega')]\, d\Omega' + \frac{1}{\pi}\int_{2\pi_+} \Gamma(\Omega' \rightarrow \Omega)I^0(\tau, \Omega')\, d\Omega'. \quad (10)$$

It is obvious that no closed-form solution to (9) can be derived. The following section will be mainly devoted to deriving the approximate formulae of $I^M(\tau, \Omega)$ using asymptotic theory as well as the analytic formula of $I^1(\tau, \Omega)$.

III. Development of the Parametric Canopy BRDF Model

In the previous section, the canopy radiative transfer equations, boundary conditions, and their solutions have been discussed. However, the multiple-scattering component has to be calculated using an iteration technique, and numerical integration is required to evaluate the upwelling single-scattering component as well. For the purpose of inversion, the solution should be as explicit and simple as possible. In the following, we will first derive the approximation to the integration in (7), then develop the formula for the multiple-scattering calculation using the asymptotic fitting technique.

A. Explicit Formula for Upwelling Single Scattering Radiance

Let us consider the upwelling radiance just above the canopy. It follows from (7) that

$$I^1(0, \Omega) = u\int_0^{\tau_c} \exp\{-a\tau' + b[1 - \exp(-c\tau')]\}\, d\tau' \quad (11)$$

where

$$\begin{cases} a = \frac{G(\Omega_0)}{|\mu_0|} + \frac{G(\Omega)}{|\mu|} & b = \sqrt{\frac{G(\Omega_0)G(\Omega)}{|\mu_0|\,|\mu|}}\frac{kH}{\Delta(\Omega_0, \Omega)} \\ c = \frac{\Delta(\Omega_0, \Omega)}{kH} & u = \frac{\Gamma(\Omega_0, \Omega)i_0}{\pi\mu}. \end{cases} \quad (12)$$

Substituting $y = \exp(-c\tau')$ for τ' associated with above equation leads to

$$I^1(0, \Omega) = -\frac{u\exp(b)}{c}\int_1^{y_0} y^{\frac{a}{c}-1}\exp(-by)\, dy \quad (13)$$

where $y_0 = \exp(-c\tau_c)$. Simulations show that c is greater than 1 and b is much smaller than 1 in most directions except in the hotspot region, where $\Delta(\Omega_0, \Omega)$ approaches zero. Expanding exponents in (13) and taking the first two terms, (13) becomes

$$I^1(0, \Omega) = u\exp(b)\left[\frac{1}{a} - \frac{b}{a+c} + \frac{b^2}{2(a+2c)}\right]. \quad (14)$$

Further analysis indicates that the third term in the bracket on the right side of this equation mainly contributes to the hotspot component.

B. Multiple Scattering Approximation

In the visible bands, the multiple-scattering component is very small, typically 5%. However, it becomes over 50% of the total upwelling radiance in the near-IR bands. In this spectral region, the single-scattering albedo is very large, and the optical depth is not small. Thus it seems reasonable to use asymptotic theory to approximate the multiple-scattering component.

Our previous numerical results show that the multiple-scattering component is relatively insensitive to azimuthal angles since when the canopy becomes thicker optically, the photons will scatter more times before emerging from the canopy. Also it seems that the multiple-scattering radiance distribution probably approaches the isotropic case. However, our results in a series of calculations show that the isotropic scattering function will cause large errors when there are a number of horizontal leaves in the canopy, such as in a planophile, or spherical canopy. Instead, a Henyey–Greenstein scattering phase function for the multiple-scattering and independent radiance of azimuth angles are assumed in this study. Although the Henyey–Greenstein function is an approximation to the real phase function, and will cause some errors, the single-scattering radiance is still evaluated using the exact phase function. As a result, this formulation still can predict accurately the angular dependence of the reflectance.

The asymptotic solution for a finite-thick medium with an arbitrary scattering phase function has been derived for many years [22]. If the canopy is dense with a thick optical thickness τ_c and black soil is assumed, the upwelling radiance is given by

$$\tilde{I}(0, \mu, \mu_0) = R_0(\tau_c, \mu, \mu_0)|\mu_0|i_0/\pi \quad (15)$$

where the reflectance can be calculated using the classic asymptotic theory [23]:

$$R_0(\tau_c, \mu, \mu_0) = R_\infty(\mu, \mu_0) - \frac{mf}{1-f^2}\exp(-\kappa\tau_c)E(\mu)E(|\mu_0|). \quad (16)$$

$R_\infty(\mu, \mu_0)$ is the reflectance function of a semi-infinite canopy, and $E(\mu)$ is the escape function. To account for the soil reflectance, the classic reflectance formula in the case of a Lambertian soil is

$$\tilde{R}_0(\tau_c, \mu, \mu_0) = R_0(\tau_c, \mu, \mu_0) + \frac{r_s}{1 - r_s A^*}t_0(\tau_c, \mu)t_0(\tau_c, \mu_0) \quad (17)$$

where r_s is the soil Lambertian reflectance, $t_0(\tau_c, \mu)$ is the diffuse transmittance, and A^* is the spherical albedo of the canopy.

With some algebraic manipulation, a more simplified formula considering the back-ground reflectance has been derived on the basis of above relations by King [24]

$$\tilde{R}_0(\tau_c, \mu, \mu_0) = R_\infty(\mu, \mu_0) - \frac{mG(r_s)E(\mu)E(|\mu_0|)}{\exp(2\kappa\tau_c) - lG(r_s)} \quad (18)$$

where $G(r_s)$ is defined as

$$G(r_s) = l - \frac{mn^2 r_s}{1 - r_s A^*}. \quad (19)$$

Although the above formula originally is for a thick cloud, its derivations are also valid for the canopy, and the same results can be derived. If $r_s = 0$, then (18) is equivalent to (16). Notice that $f = l\exp(-\kappa\tau_c)$.

The parameters κ, l, n, and m have been correlated with the similarity parameter s, defined in terms of the single-scattering albedo ω_c and the scattering asymmetry factor g_c of the One-Term Henyey–Greenstein (OTHG) scattering phase function as

$$s = \sqrt{\frac{1 - \omega_c}{1 - \omega_c g_c}}. \quad (20)$$

King and Harshvardhan [25] give the following results:

$$\begin{aligned}
\kappa &= \sqrt{3}s - \frac{(0.985 - 0.253s)s^2}{6.464 - 5.464s}, \\
l &= \frac{(1 - 0.681s)(1 - s)}{1 + 0.792s}, \\
n &= \sqrt{\frac{(1 + 0.414s)(1 - s)}{1 + 1.888s}}, \\
m &= (1 + 1.537s)\ln\left[\frac{1 + 1.8s - 7.087s^2 + 4.74s^3}{(1 - 0.819s)(1 - s)^2}\right].
\end{aligned} \quad (21)$$

The spherical albedo is estimated by van de Hulst [23]:

$$A^* = \frac{(1 - 0.139s)(1 - s)}{1 + 1.17s}. \quad (22)$$

The semi-infinite reflectance and the escape function are employed using look-up table procedures. The tabular data are taken from van de Hulst [23] and stored in the computer. The linear interpolation method is used to produce the corresponding values. In fact, the escape function $E(\mu)$ was fitted by Yi *et al.* [26]

$$E(\mu) = A(\mu) + B(\mu)(1 - s) + C(\mu)(1 - s)^2 + D(\mu)(1 - s)^3 \quad (23)$$

where the coefficients are

$$\begin{aligned}
A(\mu) &= -1.113 + 5.3924\mu - 9.1658\mu^2 + 5.4673\mu^3 \\
B(\mu) &= 5.9551 - 26.488\mu + 46.782\mu^2 - 25.743\mu^3 \\
C(\mu) &= -8.7748 + 43.229\mu - 73.949\mu^2 + 39.059\mu^3 \\
D(\mu) &= 4.3639 - 21.230\mu + 36.285\mu^2 - 18.799\mu^3.
\end{aligned} \quad (24)$$

Although the polynomials for the escape function $E(\cdot)$ are fitted from data with $\omega_c \geq 0.8$, $0.8 \leq g_c \leq 0.9$, and $\mu \geq 0.5$, they do not produce results that are significantly different from the tabular data for the canopy problem.

The above formulae determine the reflectance of all orders of scattering. In order to account for the hotspot effect and the dependence of the total reflectance on azimuth angle, the exact single-scattering component should be used. Thus, the multiple-scattering reflectance in (15) can be obtained through subtracting the azimuth-independent single-scattering component from (18):

$$\tilde{R}_0^M(\tau_c, \mu, \mu_0) = \tilde{R}_0(\tau_c, \mu, \mu_0) - \frac{\omega_c p_c(\mu, \mu_0)}{4(\mu + |\mu_0|)}\left[1 - \exp\left(-\frac{\mu + |\mu_0|}{|\mu_0|\mu}\tau_c\right)\right] \quad (25)$$

where the $p_c(\mu, \mu_0)$ is the azimuth-independent part of the Henyey–Greenstein function $\Phi(\cdot)$:

$$p_c(\mu, \mu_0) = \frac{1}{2\pi}\int_0^{2\pi} \Phi[\mu\mu_0 + \sqrt{(1 - \mu^2)(1 - \mu_0^2)}\cos\phi]\, d\phi. \quad (26)$$

The total canopy BRDF becomes the sum of the exact single-scattering term plus the unscattered sunlight reflectance term normalized by the incident radiation and the approximate multiple-scattering component:

$$R(\tau_c, \Omega, \Omega_0) = \frac{I^1(0, \Omega, \Omega_0) + I^0(0, \Omega, \Omega_0)}{|\mu_0| i_0} + \frac{\tilde{R}_0^M(\tau_c, \mu, \mu_0)}{\pi}. \quad (27)$$

IV. Modeling Downward Sky Radiance Distribution

The previous section considers only the collimated (direct) incident radiation. However, canopies always are illuminated by both direct solar radiance and diffuse sky radiance in the natural environment. For such a case, the upwelling radiance above the surface should be

$$L(\tau_a, \Omega) = \int_0^{2\pi}\int_{-1}^{0} [R(\tau_c, \Omega, \Omega_i)[I^s(\tau_a, \Omega_i) + I^0(\tau_a, \Omega_i)\delta(\Omega_i - \Omega_0)]|\mu_i|]\, d\Omega_i \quad (28)$$

where $I^0(\tau_a, \Omega_0)$ is the direct solar radiance, $I^s(\tau_a, \Omega_i)$ is the scattered downward radiance, $R(\tau_c, \Omega, \Omega_i)$ is the canopy BRDF defined by (27), and τ_a is the atmospheric optical depth.

The upwelling radiance can be measured by hand-held radiometers with small solid-angle fields of view. It is evident that we need to know the sky radiance distribution in order to retrieve relevant parameters from measured radiances. Some instruments can measure both the upwelling radiance and the downward sky radiance simultaneously (e.g., PARABOLA [27]), but most cannot. In the following, we discuss a sky radiance model for the case that sky radiances are not measured.

Attempts to describe the angular distribution of the sky radiance have generally followed three approaches. In the first approach, the radiative transfer equation is solved using various numerical techniques [15]. For the sake of the inversion where rapid inversion is the goal, this approach is not practical since the iterative solution process is computationally quite expensive. An alternative approach is to use a statistical

technique to fit collected sky radiance data. Some models have been proposed over the years, for example, those for overcast skies [28], [29]. The third approach is to derive approximate formulae based on a radiative transfer equation. For example, Sobolev [30] provides an Eddington-type approximation formula, which was found to be quite accurate through comparison with field measurements [31]. Verhoef [32] presents a four-stream approximation for the scene modeling. Another double-scattering sky radiance model has been used for the data analysis of the component parabolic concentrating collector based on the successive-order-of-scattering principle [33]. Some popular codes such as LOWTRAN [34] and 5S [35] are based on two-stream approximations using this approach. This type of model is well suited to the present study. However, most of these models are developed mainly for radiative flux calculations.

In the following, we will briefly describe a new formulation for calculating the sky radiance distribution based on the two-stream approximation of atmospheric radiative transfer for the multiple-scattering calculation. For a plane-parallel homogeneous atmosphere in the absence of clouds and polarization, the radiative transfer equation can be written as [36]

$$\mu\frac{\partial I_a(\tau,\,\Omega)}{\partial\tau} = I_a(\tau,\,\Omega) - \frac{\omega_a}{4\pi}\int_{4\pi} P(\Omega',\,\Omega)I_a(\tau,\,\Omega')\,d\Omega' \tag{29}$$

with the boundary conditions

$$\begin{aligned} I_a(0,\,\Omega) &= \delta(\Omega-\Omega_0)\pi F_{a0} \\ I_a(\tau_a,\,\Omega) &= \int_{2\pi_-} R(\Omega',\,\Omega)|\mu'|I_a(\tau_a,\,\Omega')\,d\Omega' \end{aligned} \tag{30}$$

where ω_a is the atmospheric single-scattering albedo, $P(\Psi)$ is the phase scattering function, and $R(\Omega',\,\Omega)$ is the canopy BRDF defined in (27). The scattering properties of the atmosphere are taken to depend on Rayleigh molecular and aerosol particles, and the scattering phase function is thus defined as the weighted average of individual scattering phase functions where the aerosol phase function takes the one-term Henyey–Greenstein (OTHG) function.

To provide an accurate characterization of the angular distribution of the sky radiance, the radiation field is divided into three parts, as for the canopy: unscattered solar radiance, single-scattering radiance, and multiple-scattering radiance. Here, we do not give the corresponding equations and boundary conditions; interested readers are referred to our previous paper [10]. For the first two components, their downward radiances are

$$\begin{aligned} I_a^0(\tau_a,\,\Omega) &= \pi F_{a0}\exp\left(-\frac{\tau_a}{|\mu_0|}\right)\delta(\Omega-\Omega_0) \\ I_a^1(\tau_a,\,\Omega) &= \frac{|\mu_0|F_{a0}\omega_a P(\Psi)}{4(|\mu_0|-|\mu|)} \\ &\quad\cdot\left[\exp\left(-\frac{\tau_a}{|\mu_0|}\right)-\exp\left(-\frac{\tau_a}{|\mu|}\right)\right] \qquad \mu\neq\mu_0 \\ I_a^1(\tau_a,\,\Omega) &= \frac{\omega_a F_{a0}\tau_a}{4|\mu_0|}P(\Psi)\exp\left(-\frac{\tau_a}{|\mu_0|}\right) \qquad \mu=\mu_0. \end{aligned} \tag{31}$$

For the multiple-scattering calculation, the two-stream approximation is applied where only the azimuthal-integrated radiance will be dealt with $I_a(\tau,\,\mu)=\int_0^{2\pi} I_a(\tau,\,\mu,\,\phi)\,d\phi$. By defining the hemispherical integrals

$$\begin{aligned} I^+(\tau) &= \int_0^1 \mu I_a(\tau,\,\mu)\,d\mu \\ I^-(\tau) &= \int_{-1}^0 |\mu| I_a(\tau,\,\mu)\,d\mu \end{aligned} \tag{32}$$

where $\pm$ stands for upward $(+)$ and downward $(-)$ directions, respectively, the radiative transfer equations become [37]

$$\begin{aligned} \frac{dI^+}{d\tau} &= \gamma_1 I^+ - \gamma_2 I^- - \pi F_{a0}\omega_a\gamma_3\exp\left(-\frac{\tau}{|\mu_0|}\right) \\ \frac{dI^-}{d\tau} &= \gamma_2 I^+ - \gamma_1 I^- + \pi F_{a0}\omega_a(1-\gamma_3)\exp\left(-\frac{\tau}{|\mu_0|}\right). \end{aligned} \tag{33}$$

Meador and Weaver [37] showed that the differences among various two-stream approximations are due to their definitions of coefficients γ_1–γ_3. Here we accept the hybrid modified Eddington-delta approximation [37], which has been proven to be generally superior to other two-stream approximations over a wide range of atmosphere conditions. The parameters are

$$\begin{aligned} \gamma_1 &= \frac{7-3g^2-\omega_a(4+3g)+\omega_a g^2(4\beta+3g)}{4[1-g^2(1-|\mu_0|)]} \\ \gamma_2 &= \frac{g^2-1+\omega_a(4-3g)+\omega_a g^2(4\beta+3g-4)}{4[1-g^2(1-|\mu_0|)]} \\ \gamma_3 &= \beta \end{aligned} \tag{34}$$

where $g=\tau_{ae}g_a/(\tau_{ae}+\tau_r)$, g_a is the parameter of the OTHG function, τ_{ae} and τ_r are the aerosol and Rayleigh optical depth, respectively. β is the backscatter fraction, defined as

$$\beta = \frac{1}{2}\int_0^1 p(|\mu_0|,\,-\mu')\,d\mu' \tag{35}$$

where $p(\mu,\,\mu')=\frac{1}{2\pi}\int_0^{2\pi} P(\mu,\,\phi,\,\mu',\,\phi')\,d\phi$.

Meador and Weaver [37] provide the solutions to (33) for the case of an absorbing boundary condition (black surface). However, in this study, we have to consider the canopy reflectance. It is very difficult to use an arbitrary BRDF as the boundary condition to obtain the explicit solution. Instead, the spherical albedo ρ of the canopy, which can be calculated by the canopy BRDF defined in (27), is used to represent the canopy reflectance. Thus, the boundary conditions for (33) are

$$\begin{aligned} I^-(0) &= 0 \\ I^+(\tau_a) &= \rho[I^{-1}(\tau_a)+\pi F_0|\mu_0|\exp(-\tau_a/|\mu_0|)]. \end{aligned}$$

Note that this simplification is used only for the multiple-scattering calculation. The tedious derivation procedures are omitted here, and the final solutions are

$$\begin{aligned} I^+(\tau) &= X_1\exp(\eta\tau)+X_2\exp(-\eta\tau)+X_3\exp\left(-\frac{\tau}{|\mu_0|}\right) \\ I^-(\tau) &= \frac{1}{\gamma_2}\left[(\gamma_1-\eta)X_1\exp(\eta\tau)+(\gamma_1+\eta)X_2\exp(-\eta\tau)\right. \\ &\quad \left.+t_0\exp\left(-\frac{\tau}{|\mu_0|}\right)\right] \end{aligned} \tag{36}$$

where X_i $(i = 1, 2, 3)$ are defined as

$$X_1 = \frac{t_0 w_2 - w_0(\gamma_1 + \eta)}{(\eta + \gamma_1)w_1 + (\eta - \gamma_1)w_2}$$
$$X_2 = -\frac{t_0 w_1 - w_0(\gamma_1 - \eta)}{(\eta + \gamma_1)w_1 + (\eta - \gamma_1)w_2}$$
$$X_3 = \frac{\pi F_{a0}\omega_a\left(\gamma_1\gamma_3 + \gamma_2\gamma_4 - \frac{\gamma_3}{|\mu_0|}\right)}{\eta^2 - \frac{1}{\mu^2}}. \quad (37)$$

Other parameters are given by

$$t_0 = \left(\gamma_1 + \frac{1}{|\mu_0|}\right)X_3 - \pi F_{a0}\omega_a\gamma_3$$
$$w_0 = \left\{\left[\rho\left(\gamma_1 + \frac{1}{|\mu_0|}\right) - \gamma_2\right]X_3 + \pi F_{a0}\rho(|\mu_0| - \omega_a\gamma_3)\right\}\exp\left(-\frac{\tau_a}{|\mu_0|}\right)$$
$$w_1 = [\rho(\gamma_1 - \eta) - \gamma_2]\exp(\eta\tau_a)$$
$$w_2 = [(\gamma_1 + \eta)\rho - \gamma_2]\exp(-\eta\tau_a)$$
$$\eta = \sqrt{\gamma_1^2 - \gamma_2^2}. \quad (38)$$

If ρ is equal to 0, then the above formulae are equivalent to those of Meador and Weaver. Thus, the total approximate downward scattering radiance at any arbitrary direction is $(\mu < 0)$:

$$\hat{I}_a(\tau_a, \mu) = \frac{1}{1 - g^2(1 - |\mu_0|)} \cdot[(1 - g^2)T + g^2\delta(\mu - \mu_0)I^-(\tau_a)] \quad (39)$$

where T is defined as

$$T = (1 + 1.5\mu)I^+(\tau_a) + (1 - 1.5\mu)I^-(\tau_a).$$

The multiple-scattering downward radiance is the total approximate radiance less the approximate single-scattering radiance

$$I_a^M(\tau_a, \mu) = \hat{I}_a(\tau_a, \mu) - \hat{I}_a^1(\tau_a, \mu). \quad (40)$$

For $\hat{I}_a^1(\tau_a, \mu)$, the second term of the right side of (29) is zero. Thus we could have the same equation as (33) except that γ_1 and γ_2 must be replaced by γ_1' and γ_2' defined as

$$\gamma_1' = \frac{7 - 3g^2}{4[1 - g^2(1 - |\mu_0|)]}$$
$$\gamma_2' = \frac{g^2 - 1}{4[1 - g^2(1 - |\mu_0|)]}. \quad (41)$$

Other formulas are the same as those of $\hat{I}_a(\tau_a, \mu)$. Notice that the spherical albedo ρ needs to be set zero for $\hat{I}_a^1(\tau_a, \mu)$. Thus, the total downward sky radiance becomes

$$I_a(\tau_a, \Omega) = I_a^1(\tau_a, \Omega) + I_a^M(\tau_a, \mu)/2\pi. \quad (42)$$

It is possible to incorporate a δ-function adjustment to account for the forward scattering peak in the context of the two-stream approximation [38]. If a fraction of the scattering energy f is considered to be in the forward peak, the above formulas can still be used as long as the following transformations are made in the coefficients:

$$\tau_a \to \tau_a' = (1 - \omega_a f)\tau_a$$
$$\omega_a \to \omega_a' = \frac{(1 - f)\omega_a}{1 - \omega_a f}$$
$$g_a \to g_a' = \frac{g_a - f}{1 - f}. \quad (43)$$

Although various choices of f are possible, the most frequently used choice [38], and the one used in all computational results to be presented below, is $f = g_a^2$.

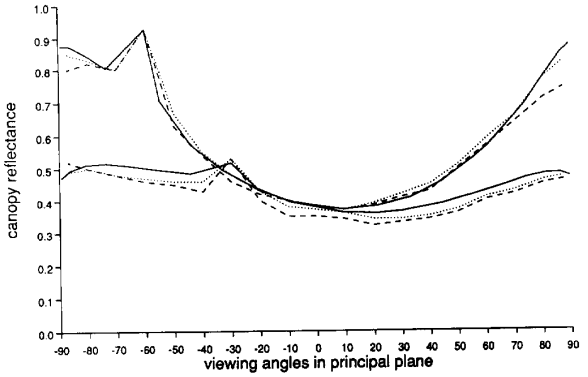

Fig. 2. Comparisons of the present analytic canopy model with Monte Carlo models. The solid curves stand for the analytic model, the dotted curves for the Antyufeev–Marshak model, and the dashed curves for Ross–Marshak model. Here $r_l = t_l = 0.46$, $r_s = 0.2$, $LAI = 3.0$, $k = 0.08$, $\phi_0 = 0°$, erectophile canopy, $\theta_0 = 60°$ for the upper set of curves, $\theta_0 = 30°$ for the lower set of curves, $g_c = 0.08$.

V. Model Validations

To evaluate the accuracies and analyze the behaviors of the analytic BRDF leaf-canopy model and the sky radiance distribution model, a series of validations have been carried out. For the canopy model, Monte Carlo methods [39], [40] and the discrete-ordinates method [19] are used to test the accuracy of the present model. Fig. 2 compares our analytic calculations with two Monte Carlo methods for an erectophile canopy (mainly vertical leaves). There is a good agreement among these three models.

Fig. 3 provides another comparison of our analytic model to the Antyufeev–Marshak model [39] for a planophile canopy (mainly horizontal leaves). Our model overestimates reflectance somewhat when the viewing angles are greater than 55°.

Fig. 4 demonstrates the comparison for a spherical canopy (leaves randomly distributed) calculation with the discrete-ordinates model of Marshak [19]. Three sets of curves stand for different azimuth directions. This comparison also confirms that our model predicts reflectance well for different azimuth directions. Compared with numerical models, this model has reduced the computation significantly.

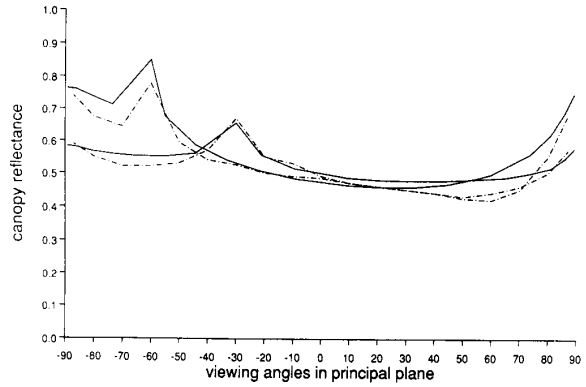

Fig. 3. Comparisons of the present analytic canopy model with a Monte Carlo model. The solid curves stand for the present model, and the dot–dashed curves for the Antyufeev–Marshak model. Planophile canopy, $g_c = 0.1$; other parameters are as in Fig. 2.

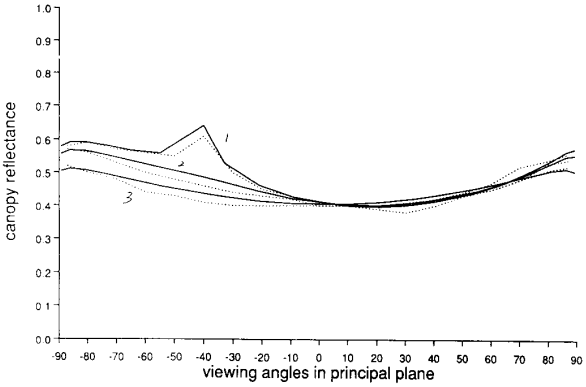

Fig. 4. Comparisons of the present analytic canopy model with a discrete-ordinates model. The solid curves stand for the analytic model, and the dot–dashed curves for the Marshak model [19, fig. 6]. 1 stands for $\phi = \phi_0$ and $\phi = \phi_0 + 180°$, 2 for $\phi = \phi_0 + 45°$ and $\phi = \phi_0 + 225°$, and 3 for $\phi = \phi_0 + 90°$ and $\phi = \phi_0 + 270°$. Uniform canopy, $LAI = 4.0$, $\theta_0 = 40°$, $\phi_0 = 100°$, $g_c = 0.15$, other parameters are the same as Fig. 2.

The analytic sky radiance-distribution model was validated using the DISORT discrete-ordinate code [41]. Fig. 5 compares our analytic model with the numerical model for aerosol scattering above a Lambertian surface. If the aerosol optical depth is smaller than 0.2, our analytic model is quite accurate, especially when the zenith angle is smaller than 75°. Note that if the sky is clear, the aerosol optical depth is usually smaller than 0.2 in the near-infrared region. Although only one set of results is presented here, other calculations validate this conclusion.

VI. Inversion Algorithm and Data Analysis

Having validated the canopy BRDF and the sky radiance distribution models against more exact calculations, the remaining issue is how to invert these models from measured directional data to provide estimates of biophysical parameters. As in ordinary inversion studies [3], an optimum technique will be used to invert them through minimizing a merit function

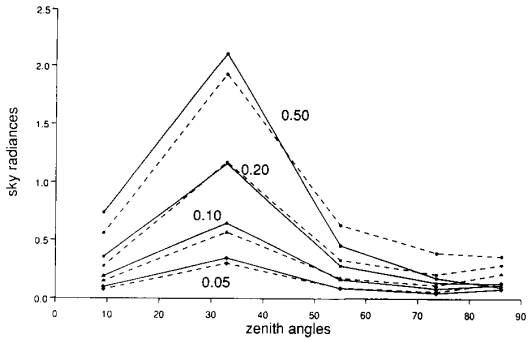

Fig. 5. Validation of the sky radiance distribution model using the numerical discrete-ordinates algorithm for the aerosol atmosphere. The solid lines stand for our model, and the dashed lines for the numerical model. $\theta_0 = 30$, azimuth angle $\phi = \phi_0 = 0$, $g_a = 0.73$, $r_s = 0.2$, $\omega_a = 0.9$. The numbers labeled in the figure are the aerosol optical depths.

$F(\Psi_a, \Psi_b)$ consisting of the sum of squares of the residuals and a penalty function

$$F(\Psi_A, \Psi_B) = \sum_{k=1}^{K} w_k [I_k - \hat{I}_k(\Psi_A, \Psi_B)]^2 + f(\Psi_A, \Psi_B) \tag{45}$$

where w_k's are weight factors, I_k is the measured radiance, $\hat{I}_k(\Psi_A, \Psi_B)$ is the predicted radiance by models with canopy BRDF parameters Ψ_A and atmosphere parameters Ψ_B, and $f(\Psi_A, \Psi_B)$ is the penalty function, which keeps estimated parameters or their functions in reasonable bounds. In this study, the beta function [42] is employed to represent the leaf angle distribution, which contains two parameters u and v. Thus, the parameter set Ψ_A includes

LAI	leaf area index;
r_l	leaf reflectance;
t_l	leaf transmittance;
u and v	LAD parameters;
k	leaf dimension parameter;
n	leaf wax refractive index;
g_c	asymmetry parameter of Henyey–Greenstein phase function for the canopy multiple-scattering calculation;
r_s	soil Lambertian reflectance.

The atmospheric parameter set Ψ_B includes:

τ_a	aerosol optical depth;
g_a	asymmetric parameter of Henyey–Greenstein phase function for the aerosol;
ω_a	aerosol single-scattering albedo;
τ_r	Rayleigh optical depth

where τ_r usually can be treated as a constant at a specific wavelength.

The construction of the penalty function is simple. Based on constraint functions, say, $g_i(\Psi_A, \Psi_B) > 0$, the Siddall algorithm [43] is

$$f(\Psi_A, \Psi_B) = 10^{20} \sum_{\hat{I}} |g_i(\Psi_A, \Psi_B)| \tag{46}$$

where $\hat{I}$ identifies the set of violated constraints, that is

$$g_i(\Psi_A, \Psi_B) < 0 \tag{47}$$

for all i in $\hat{I}$. The constraint function comes from a series of constraints on either individual parameters or their functions. For example, the single-scattering albedo ω should be $0 \leq \omega \leq 1$. The spherical albedo of the canopy ρ should be $0 < \rho < 1$. If the atmosphere parameters Ψ_B are known, then only BRDF parameters are to be estimated.

In order to find optimal estimates of these parameters, an iteration process is necessary. At each iteration, the iteration length and iteration direction need to be determined. To date, the most successful direct search algorithm is the method due to Powell [44], especially with the modifications suggested by Zhangwill [45] and Brent [46], which we will refer to as the Powell algorithm. One of the best features of this algorithm is that we do not need to derive the derivatives of the merit function, which is often very difficult. Thus, we can incorporate any type of penalty function to yield realistic solutions. This algorithm has been recently used for inversion of canopy parameters by Kuusk [47].

To test the inversion procedure, the models are used to calculate several sets of noise-free directional data, each with 60 angles in the reflectance hemisphere. In all attempts, the inversion program converges to the true parameters, demonstrating that our models are mathematically totally invertible, as discussed in Goel [48]. However, real measured data will contain noise to some extent. As a further test, we ran the inversion program for the soybean reflectance data measured by Ranson *et al.* [16], which have been widely applied in inversion research. We selected the near-infrared data (800–1100 nm) measured on August 17, 1980 because on that date the canopy was completely closed and exhibited minimal row structure, so that the homogeneous assumption for the canopy is valid. To fit the model to these data, atmospheric conditions must be specified. The extraterrestrial solar irradiance data are from [49]. A correction factor accounting for the variation of the sun-earth distance is taken from Iqbal's tabular data [50]. Since the atmospheric parameters were not measured, we selected reasonable values for moderately clear air: $\omega_a = 0.95$, $g_a = 0.75$, $\tau_{ae} = 0.02$, $\tau_r = 0.012$, for band 4. The upwelling radiance above the canopy is normalized to give the reflectance

$$R(\Omega) = \frac{I(0, \Omega)}{|\mu_0| F_0 \exp(-\tau_a/|\mu_0|) r_0}$$

where r_0 is the reflectance of a Lambertian panel.

In our tests, we selected four of the nine free canopy parameters: LAI, LAD parameters u and v, and g_c. Other parameters are set to the measured values. As the leaf dimensional parameter k and leaf wax refractive index n were not measured, we arbitrarily set $k = 0.05$, and $n = 1.2$. To reduce the computational requirements, we first inverted g_c, then retrieved LAI, u and v. Further, reflectances of viewing angle $\theta = 60°$ are not used in the inversion. Another reason that we did not use the reflectance of 60° viewing angle is that this model is most accurate at smaller viewing angles, as shown in the validations. All weight factors w_i are set at unity. The results are summarized in Table I.

TABLE I
INVERSION RESULTS FOR THE SOYBEAN DATA

Data Set #	θ_0	ϕ_0	Retrieved Values			
			LAI	u	v	g_c
c1	38	136	2.831	2.786	2.767	0.172
c2	35	145	2.851	2.796	3.846	0.168
c3	32	163	2.856	3.950	8.674	0.174
c4	31	174	2.867	5.050	10.001	0.164
c5	31	196	3.024	3.013	8.227	0.120
c6	33	206	3.086	3.067	8.845	0.109
c7	36	217	2.877	2.721	5.011	0.103
c8	38	225	3.041	3.504	9.825	0.114
c9	44	237	2.971	3.907	8.309	0.123
c10	48	243	3.090	3.757	8.210	0.143
c11	55	251	2.893	2.922	3.875	0.140
c12	61	258	2.895	2.078	2.839	0.150
Measured value			2.90	1.806	2.447	

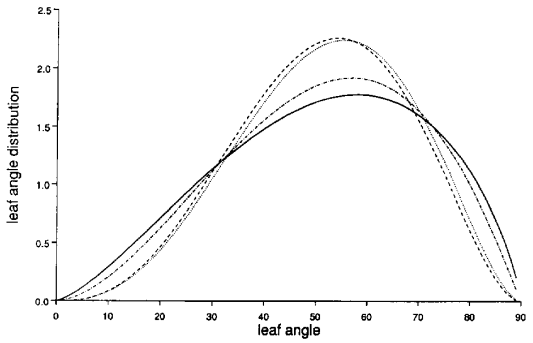

Fig. 6. Illustrations of measured (solid curve) and retrieved LAD at different solar positions (dot–dashed curve for c12, dashed curve for c11, and dotted curve for c1).

From the table, we can observe that LAI is very accurately inverted, but u and v depart somewhere from the measured data. When the measured and retrieved parameters are presented as leaf angle distributions (Fig. 6), they are surprisingly similar for some data sets such as c2, c11, c12, in spite of the numerical differences in parameter values. However, there are larger deviations from other data sets. In a series of inversions, Goel and his colleagues found that LAD cannot be accurately inverted from Suits model and/or SAIL model, although the average leaf angle can be well inverted [51]. Kuusk [47] also found that Nilson–Kuusk model cannot be inverted well in the near-IR region, where the multiple-scattering component dominates. However, we think that one of the major reasons that not all LAD's can be correctly inverted is that the soybean directional reflectance data do not contain hotspot measurements. These were deliberately omitted, due to the sensing of the shadow of the instrument.

VII. DISCUSSION

Before finishing this paper, we would like to discuss several issues associated with the above models.

1) *Canopy phase function*: Theory and experiments have shown that the canopy phase function is rotationally variant. That means that the scattering function depends not only on the phase angle, but also on the

absolute incidence and outgoing directions. Therefore, a rotationally invariant transfer phase function such as the Henyey–Greenstein function is inappropriate for the canopy problem. In earlier modeling efforts, it has often been used due to its simplicity. In the present work, it is only used for the multiple-scattering calculation, while the single-scattering calculation still is based on the exact rotationally-variant phase function. In principle, the asymmetry factor g_c of the Henyey–Greenstein function is not an independent variable, and can be determined by other variables such as r_l, t_l, n, k, and so on. However, it is difficult to relate g_c to those variables, especially in the inversion program. With the additional variable g_c, the inversion efficiency greatly improves. In the atmospheric radiative transfer, the asymmetric factor is usually greater than 0.60. Fig. 7 illustrates the phase function with different g values. The smaller the factor, the larger the backscattering component. It intuitively seems reasonable if the canopy has larger backscattering than aerosol.

2) *Coupling of the atmosphere and canopy*: Although both the atmosphere and canopy are parameterized by asymptotic theory and the two-stream approximation in this study, a consistent approximation will be preferred. The interaction between the canopy and atmosphere is illustrated in (28), in which numerical integrations are required. A 6 by 10 double-Gauss quadrature [10] is always examined in the above results. The procedures described in the above several sections are suited for ground-measured data. For airborne or spaceborne remotely sensed data, path radiance must be taken into consideration. A new formulation incorporating an non-Lambertian surface has been developed and will be discussed in a forthcoming paper [52].
3) *Computation problems*: Several factors affect the inversion speed. First, the calculation of the area-scattering transfer function of the canopy is computationally very expensive, which has been recognized by Nilson [53]. Second, the Powell algorithm is time consuming although this algorithm is quite robust in obtaining the global minimum. Another factor is the coupling between the atmosphere and canopy. It seems to us that the development of a new parameterization scheme for the calculation of the area-scattering transfer function will be also very helpful to speed to inversions.
4) *Further improvements*: First, we need to improve the inversion efficiency of this model, including (1) the consistent parameterization schema of both atmosphere and canopy, and (2) the approximation formula for the calculation of the area-scattering transfer function. Second, more examinations of the asymmetric factor g_c are required to understand its dependence on other biophysical parameters. Third, a sensitivity study is required in order to determine how many and which parameters can be retrieved effectively given a set of measurement data. The final issue is how to incorporate non-Lambertian soil reflectance into this model. In fact, this is not a critical problem for an optically thick canopy because in such a medium, the unscattered radiance becomes very small, and multiple scattering tends to smooth the angular anisotropy of the soil reflectance. In addition, there are several overlap functions accounting for the hotspot effect available [54], [11]. Comparisons of these functions in the present framework would be very helpful for us to more effectively model the canopy radiative transfer.

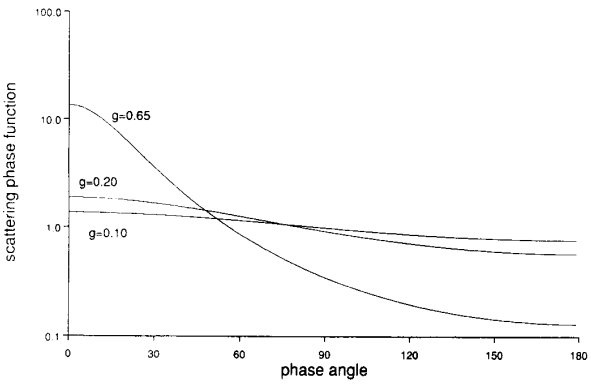

Fig. 7. Illustration of the Henyey–Greenstein function with different asymmetric parameters.

VIII. Conclusion

An analytic BRDF model of canopy radiative transfer as well as an analytic sky radiance distribution model are developed. To obtain more realistic solutions, the canopy and sky radiation fields are divided into three parts: unscattered solar radiance, single-scattering radiance, and multiple-scattering radiance. The first two components can be explicitly calculated, and the multiple-scattering component is approximated by the asymptotic technique for the canopy, and the two-stream technique for the atmosphere. Compared with other invertible canopy models, the present canopy model is uniquely based on a rigorous radiative transfer equation so that the multiple-scattering approximation can be validated using accurate numerical solutions. Also, the sky radiance distribution model is directly incorporated. The results indicate that our canopy model fits the numerical solutions and field data very well. The inversion procedure applied in this paper enables us to effectively explore the relationship between the directional reflectance of the plant canopy and the biophysical parameters that control it.

Acknowledgment

The authors would like to thank Dr. X. Li for his careful reading of the mathematical portion of the manuscript and making many comments and corrections, and Dr. M. Verstraete for his thought-provoking comments. Dr. W. Wiscombe kindly provided the authors with the atmospheric radiative transfer code DISORT.

REFERENCES

[1] J. R. Irons, K. J. Ranson, D. L. Williams, R. R. Irish, and F. G. Huegel, "An off-nadir pointing imaging spectroradiometer for terrestrial ecosystem studies," *IEEE Trans. Geosci. Remote Sensing*, vol. 29, pp. 66–74, 1991.

[2] D. J. Diner, C. J. Bruegge, J. V. Martonchik, T. P. Ackerman, R. Davies, S. A. W. Gerstl, H. R. Gordon, P. J. Sellers, J. Clark, J. A. Damiels, E. D. Danielson, V. G. Duval, K. P. Klaasen, G. W. Lilienthal, D. I. Nakamoto, R. J. Pagano, and T. H. Reilly, "MISR: A multiangle imaging spectroradiometer for geophysical and climatological research for EOS," *IEEE Trans. Geosci. Remote Sensing*, vol. 27, pp. 200–214, 1989.

[3] N. S. Goel, "Models of vegetation canopy reflectance and their use in estimation of biophysical parameters from reflectance data," *Remote Sens. Rev.*, vol. 4, pp. 1–222, 1988.

[4] R. B. Myneni, J. Ross, and G. Asrar, "A review on the theory of photon transport in leaf canopies," *Agric. For. Meteorol.*, vol. 45, pp. 1–153, 1990.

[5] G. W. Suits, "The calculation of the directional reflectance of a vegetative canopy," *Remote Sens. Environ.*, vol. 2, pp. 117–125, 1972.

[6] W. Verhoef, "Light scattering by leaf layers with application to canopy reflectance modeling: The SAIL model," *Remote Sens. Environ.*, vol. 16, pp. 125–141, 1984.

[7] P. Camillo, "A canopy reflectance model based on an analytical solution to the multiple-scattering equation," *Remote Sens. Environ.*, vol. 23, pp. 453–477, 1987.

[8] B. Pinty and M. M. Verstraete, "Extracting information on surface properties from bidirectional reflectance measurements," *J. Geophys. Res.*, vol. 96, pp. 2865–2874, 1991.

[9] T. Nilson and A. Kuusk, "A reflectance model for the homogeneous plant canopy and its inversion," *Remote Sens. Environ.*, vol. 27, pp. 157–167, 1989.

[10] S. Liang and A. H. Strahler, "Calculation of the angular radiance distribution for a coupled atmosphere and canopy," *IEEE Trans. Geosci. Remote Sensing*, vol. 31, pp. 491–502, 1993.

[11] M. M. Verstraete, B. Pinty and R. E. Dickinson, "A physical model of the bidirectional reflectance of vegetation canopies, 1. Theory," *J. Geophys. Res.*, vol. 95, pp. 11,755–11,765, 1990.

[12] B. Pinty, M. M. Verstraete and R. E. Dickinson, "A physical model of the directional reflectance of vegetation canopies 2. Inversion and validation," *J. Geophys. Res.*, vol. 95, pp. 11, 767–11, 775, 1990.

[13] B. W. Hapke, "Bidirectional reflectance spectroscopy 1. Theory," *J. Geophys. Res.*, vol. 86, pp. 3039–3054, 1981.

[14] S. P. Ahmad and D. W. Deering, "A simple analytic function for bidirectional reflectance," *J. Geophys. Res.*, vol. 97, pp. 18 867–18 886, 1993.

[15] J. V. Dave, "Extensive datasets of the diffuse radiation in realistic atmospheric models aerosols and common absorbing gases," *Solar Energy*, vol. 21, pp. 361–369, 1978.

[16] K. J. Ranson, L. L. Biehl, and C. S. T. Daughtry, "Soybean canopy reflectance modeling data sets," LARS Tech. Rep. 071584, 1984.

[17] S. A. W. Gerstl and A. A. Zardecki, "Coupled atmosphere/canopy model for remote sensing of plant reflectance features," *Appl. Opt.*, vol. 24, pp. 94–103, 1985.

[18] J. Ross, *The Radiation Regime and Architecture of Plant Stands.* The Hague: Dr. W. Junk, 1981.

[19] A. L. Marshak, "The effect of the hot spot on the transport equation in plant canopies," *J. Quant. Spectrosc. Radiat. Transfer*, vol. 42, pp. 615–630, 1989.

[20] J. K. Shultis and R. B. Myneni, "Radiative transfer in vegetation canopies with an isotropic scattering," *J. Quant. Spectrosc. Radiat. Transfer*, vol. 39, pp. 115–129, 1988.

[21] R. E. Dickson, B. Pinty, and M. M. Verstraete, "Relating surface albedos in GCM to remotely sensed data," *Agricultural and Forest Meteorology*, vol. 52, pp. 109–131, 1990.

[22] H. C. Van De Hulst, "Asymptotic fitting, a method for solving anisotropic transfer problems in thick layers," *J. Comput. Phys.*, vol. 3, pp. 291–306, 1968.

[23] C. C. Van De Hulst, *Multiple Light Scattering, Tables, Formulas and Applications, vols. 1 and 2.* New York: Academic Press, 1980, p. 739.

[24] M. D. King, "Determination of the scaled optical thickness of clouds from reflected solar radiation measurement," *J. Atmos. Sci.*, vol. 44, pp. 1734–1751, 1987.

[25] M. D. King and Harshvardhan, "Comparative accuracy of selected multiple-scattering approximations," *J. Atmos. Sci.*, vol. 43, pp. 784–801, 1986.

[26] H. C. Yi, N. J. McCormick, and R. Sanchez, "Cloud optical thickness estimation from irradiance measurements," *J. Atmos. Sci.*, vol. 47, pp. 2567–2579, 1990.

[27] D. W. Deering and P. Leone, "A sphere-scanning radiometer for rapid directional measurements of sky and ground radiance," *Remote Sens. Environ.*, vol. 19, pp. 1–24, 1986.

[28] M. D. Steven, and M. H. Unsworth, "The angular distribution and interception of diffuse solar radiation below overcast skies," *Quart. J. Roy. Meteorol. Soc.*, vol. 106, pp. 57–61, 1980.

[29] F. C. Hooper and A. P. Brunger, "A model for the angular distribution of sky radiance," *ASME J. Solar Energy Eng.*, vol. 102, pp. 196–202, 1980.

[30] V. V. Sobolov, *Light Scattering in Planetary Atmospheres*, (transl. by W. M. Irvine). New York: Pergamon, 1975, p. 256.

[31] G. Zibordi and K. J. Voss, "Geometrical and spectral distribution of sky radiance: Comparison between simulation and field measurements," *Remote Sens. Environ.*, vol. 27, pp. 343–358, 1989.

[32] W. Verhoef, "A scene radiation model based on four stream radiative transfer theory," in *Proc. 3rd Int. Colloq. Signatures of Objects in Remote Sensing, (Les Ares, France)*, pp. 143–150, 1985.

[33] F. M. F. Siala and F. C. Hooper, "A model for the directional distribution of the diffuse sky radiance with an application to a CPC collector," *Solar Energy*, vol. 44, pp. 291–296, 1990.

[34] R. G. Isaacs, W. C. Wang, R. D. Worsham, and S. Goldenberg, "Multiple scattering LOWTRAN and FASCODE model," *Appl. Opt.*, vol. 26, pp. 1272–1281, 1987.

[35] D. Tanre, C. Deroo, P. Duhaut, M. Herman, J. J. Morcrette, J. Perbos, and P. Y. Deschamps, "Description of a computation code to simulate the satellite signal in the solar spectrum: The 5S code," *Int. J. Remote Sens.*, vol. 11, pp. 659–668, 1990.

[36] J. Lenoble, *Radiative Transfer in Scattering and Absorbing Atmospheres: Standard Computational Procedures.* Hampton, VA: A. Deepak, 1985.

[37] W. E. Meador and W. R. Weaver, "Two-stream approximations to radiative transfer in planetary atmospheres: A unified description of existing methods and a new improvement," *J. Atmos. Sci.*, vol. 37, pp. 630–643, 1980.

[38] J. H. Joseph, W. J. Wiscombe, and J. A. Weinman, "The delta-Eddington approximation for radiative flux transfer," *J. Atmos. Sci.*, vol. 33, pp. 2453–2459, 1976.

[39] V. S. Antyufeev and A. L. Marshak, "Monte Carlo method and transport equation in plant canopies," *Remote Sens. Environ.*, vol. 31, pp. 183–191, 1990.

[40] J. K. Ross and A. L. Marshak, "Calculation of canopy bidirectional reflectance using the Monte Carlo method," *Remote Sens. Environ.*, vol. 24, pp. 213–225, 1988.

[41] K. Stamnes, S. C. Tsay, W. Wiscombe, and K. Jayaweera, "Numerically stable algorithm for discrete-ordinate-method radiative transfer in multiple-scattering and emitting layered media," *Appl. Opt.*, vol. 27, pp. 2502–2508, 1988.

[42] N. S. Goel and D. E. Strebel, "Simple beta distribution representation of leaf orientation in vegetation canopies," *Agron. J.*, vol. 76, pp. 800–803, 1984.

[43] J. N. Siddall, *Analytical Decision-Making in Engineering Design.* Englewood Cliffs, NJ: Prentice-Hall, 1972.

[44] M. J. D. Powell, "An efficient method for finding the minimum of a function of several variables without calculating derivatives," *Computer J.*, vol. 7, pp. 155–162, 1964.

[45] W. I. Zhangwill, "Minimizing a function without calculating derivatives," *Computer J.*, vol. 10, pp. 293–296, 1967.

[46] R. P. Brent, *Algorithms for Minimizing without Derivatives.* Englewood Cliffs, NJ: Prentice-Hall, 1973.

[47] A. Kuusk, "Determination of vegetation canopy parameters from optical measurements," *Remote Sens. Environ.*, vol. 37, pp. 207–218, 1991.

[48] N. S. Goel and R. L. Thompson, "Inversion of vegetation canopy reflectance models for estimating agronomic variables. III Estimation using only canopy reflectance data as illustrated by the Suits model," *Remote Sens. Environ.*, vol. 15, pp. 223–236, 1984.

[49] H. Neckel and D. Labs, "The solar radiation between 3300 and 12500 A," *Solar Phys.*, vol. 90, pp. 205–258, 1984.

[50] M. Iqbal, *An Introduction to Solar Radiation.* New York: Academic, 1983.

[51] N. S. Goel, "Inversion of canopy reflectance models for estimation of biophysical parameters from reflectance data," in *Theory and Applications of Optical Remote Sensing*, G. Asrar, Ed. New York: John Wiley, 1989, pp. 205–251.

[52] S. Liang and A. H. Strahler, "Retrieval of surface BRDF parameters from multiangle remotely sensed data," submitted to *Remote Sens. Environ.*, 1993..

[53] T. Nilson, "Approximate analytic methods for calculating the reflectance functions of leaf canopies in remote sensing applications," in *Photon-vegetation Interactions: Applications in Optical Remote Sensing and Production Ecology.* R. B. Myneni and J. Ross, Eds. 1990, pp. 161–189.

[54] D. L. B. Jupp and A. H. Strahler, "A hotspot model for leaf canopies," *Remote Sens. Environ.*, vol. 38, pp. 193–210, 1991.

Shunlin Liang received the B.S. degree in computer cartography, the M.S. degree in remote sensing and geographic information system from Nanjing University, People's Republic of China, and the Ph.D. degree in remote sensing from Boston University, Boston, MA.

From 1986 through 1989, he was an Assistant Professor and lecturer in Nanjing University. He served as a Research Assistant in Boston University from 1989 to 1992. He is currently a postdoctoral fellow at the Center for Remote Sensing and Department of Geography, Boston University. He has published papers in marine remote sensing, image processing, and computer cartography. His present research interests focus on land surface—atmosphere radiative transfer modeling, and inversion from multiangle remotely sensed data.

Alan H. Strahler (M'86) received the B.A. and Ph.D. degrees in geography from Johns Hopkins University in 1964 and 1969, respectively.

He is currently Professor of Geography and Researcher in the Center for Remote Sensing, Boston University, Boston, MA. He has held prior academic positions at Hunter College of the City University of New York, at the University of California, Santa Barbara, and at the University of Virginia. Originally trained as a biogeographer, he has been actively involved in remote sensing research since 1978. He has been a Principal Investigator on numerous NASA contracts and grants, and is currently a member of the Science Team for the EOS MODIS instrument. His primary research interests are in spatial modeling and spatial statistics as they apply to remote sensing, and in geometric-optical modeling of remotely sensed scenes. He is particularly interested in remote sensing of forests and the inference of vegetation canopy parameters from digital images through invertible models.